

A General Sensing-assisted Channel Estimation Framework in Distributed MIMO Network

Hui Zhou *Member, IEEE*, Xiaolan Liu *Member, IEEE*, Sangarapillai Lambotharan *Senior Member, IEEE*,

Abstract—In 6G communications, it is envisioned to equip the traditional access point (AP) with sensing capability to fully benefit the existing wireless communication infrastructures. Thus, sensing-assisted communication has attracted significant attention from both industry and academia. However, most existing works focused on sensing-assisted communication in line-of-sight (LoS) scenarios due to sensing limitations, where the sensing target (ST) and communication user equipment (UE) remain the same. In this paper, we propose a general sensing-assisted channel estimation framework in the distributed multiple-input and multiple-output (DMIMO) network and consider a scenario where the ST and UE are different entities. In addition, ST is a moving target (e.g. a robot) which causes channels between APs and UEs to vary due to changes in the reflection paths of the indoor environment. Therefore, we let multiple APs to jointly sense the position of the ST, which will be incorporated in a Ray tracing model to obtain a more accurate estimate of the channels from APs to UEs for both the LoS and non-line-of-sight (NLoS) scenarios. Simulation results demonstrate that our proposed sensing-assisted communication framework achieves a much higher channel estimation accuracy and downlink throughput compared to the traditional least-square (LS) channel estimation. More importantly, the feasibility of the proposed framework has been validated to guarantee the stringent channel estimation accuracy requirement in the DMIMO network.

Index Terms—Distributed MIMO, Channel estimation, Ray tracing, Sensing-aided communication.

I. INTRODUCTION

The Joint sensing and communication (JSC) system has been recognized as a key technology to support various emerging scenarios in 6G networks, e.g., autonomous driving, digital twin, and extended reality. It enables sensing and communication to efficiently share the hardware and wireless resources in the existing communication infrastructure [1], [2]. Shifted from transmission waveform design, multiple input and multiple output (MIMO) beamforming optimization, and joint resource allocation optimization in single JSC access point (AP) scenario, the more advanced distributed MIMO (DMIMO) scenario has received significant attention recently, where multiple JSC APs are operating in the same frequency band, and time to achieve higher sensing accuracy and communication performance [2], [3]. Prior work on JSC can be mainly categorized into: 1) *sensing-assisted communication* including sensing-assisted beam tracking/training [4], [5], resource allocation and channel estimation [6]; 2) *communication-assisted*

sensing consisting of distributed/networked sensing [7], and channel state information (CSI)-enhanced sensing [8]; and 3) *joint sensing and communication* including waveform design [7], and beamforming optimization [2].

In existing works on sensing-assisted communication, the authors mainly focused on the line-of-sight (LoS) communication scenario with a single JSC AP, where the sensing target (ST) and the communication user equipment (UE) are assumed to be the same object. In [6], a MIMO radar is first deployed to measure the azimuth information of moving vehicles, which is used to develop channel estimation. Although a reflection model for millimeter wave propagation is presented for environment perception, and the non-line-of-sight (NLoS) mmWave channel can be estimated based on the information of the located reflectors [9]. The authors merely focused on the static sensing target with a single JSC AP instead of the DMIMO network. More importantly, the sensing-assisted channel estimation in a dynamic wireless environment remains unsolved.

Motivated by the above challenge, we consider a DMIMO network where the moving ST causes varying channel conditions between the APs and UEs. Due to the stringent requirement of channel estimation accuracy in the DMIMO network, we focus on enhancing the channel estimation between APs and UEs by utilizing the sensing information of the ST. Specifically, we assume that there is a dedicated sensing slot for APs to jointly perform sensing capability in each transmission frame of future 6G communications [10]. Then, the proposed sensing-assisted channel estimation framework constructs the estimated channel in a dynamic wireless environment by using the Ray-tracing method to calculate both the LoS and NLoS propagation paths. The main contributions are as follows

- Different from existing works that mainly focus on LoS scenarios with a single JSC AP, we proposed a general sensing-assisted channel estimation framework for the DMIMO network, which captures the characteristics of both the LoS path and NLoS path via the Ray-tracing technique;
- The proposed sensing-assisted channel estimation framework is able to function well in a dynamic environment instead of a static environment, which achieves a higher channel correlation coefficient and downlink throughput under various transmission power and number of APs compared to the traditional least-square (LS) channel estimation algorithm.

The rest of this letter is organized as follows. Section II presents the system model and problem formulation. Section

Hui Zhou is with Centre for Future Transport and Cities, Coventry University, U.K. (Email: hui.zhou@coventry.ac.uk).

Xiaolan Liu is with School of Electrical, Electronic and Mechanical Engineering, University of Bristol, U.K. (Email: xiaolan.liu@bristol.ac.uk).

Sangarapillai Lambotharan is with Institute for Digital Technologies, Loughborough University, U.K. (Email: S.Lambotharan@lboro.ac.uk).

III describes the sensing-assisted channel estimation framework. Section IV presents simulation results followed by the conclusions in Section V.

II. SYSTEM MODEL AND PROBLEM FORMULATION

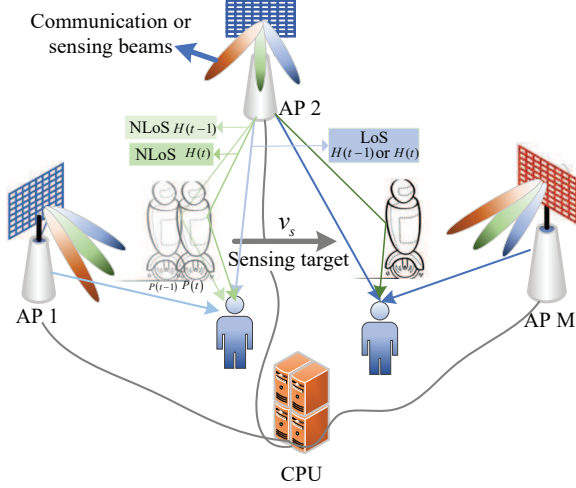


Fig. 1. System model

We consider a DMIMO JSC system with M APs, where each AP $m \in \mathcal{M} = \{1, \dots, M\}$ is equipped with N_t transmitting antennas and N_r receiving antennas in full-duplex mode. All the APs are connected to a central processing unit (CPU) that can jointly perform data processing. We assume there are U UEs, where each UE $u \in \mathcal{U} = \{1, \dots, U\}$ has N_u antennas, and one mobile ST s moving with a speed v_s towards a certain direction. It is noted that the ST is modeled as an extended target, whose length l_s and width w_s are assumed known. As shown in Fig. 1, we consider each transmission frame \mathcal{F}_j consists of N slots, i.e., $\mathcal{F}_j = \{0, \dots, N-1\}$, where the length of each slot is ΔT . In the sensing slot of each frame, i.e., $\mathcal{F}_{j,0}$, M APs operate in the monostatic radar mode, where each AP m transmits the sensing signal and receives the reflections/scattering from the ST based on full-duplex mode. In the communication slots of each frame, i.e., $\mathcal{F}_{j,\{1, \dots, N-1\}}$, all M APs serve the U UEs simultaneously [10].

A. Sensing Signal Model

We consider that each AP is equipped with a uniform linear array (ULA) [11], and transmits the signal towards the center of the ST using knowledge of the predicted position of the ST from the previous iteration in a tracking setup. We assume the K resolvable scatterers are uniformly distributed in the ST geometry. Hence, once the coordinates of these scatterers are localized, the coordinates of the centroid can be uniquely determined. In the $\mathcal{F}_{j,0}$ sensing slot, the received sensing signal at the m^{th} AP can be represented as

$$\mathbf{r}_m^{j,0}(t) = \kappa \sqrt{p_m} \sum_{k=1}^K \beta_{m,k}^{j,0} e^{j2\pi\mu_{m,k}^{j,0}t} \dots \mathbf{b}(\theta_{m,k}^{j,0}) \mathbf{a}^\dagger(\theta_{m,k}^{j,0}) \mathbf{f}^{j,0} s(t - \tau_{m,k}^{j,0}) + \mathbf{z}(t), \quad (1)$$

where $\kappa = \sqrt{N_t N_r}$ is the array gain, p_m is the transmission power, $\beta_{m,k}^{j,0}$, $\mu_{m,k}^{j,0}$ and $\tau_{m,k}^{j,0}$ represent the complex reflection coefficient, Doppler frequency, and round-trip delay of k^{th} scatter. The $\mathbf{b}(\theta_{\text{AOA}})$ and $\mathbf{a}(\theta_{\text{AOD}})$ represent the array response vector corresponding to the reception and transmission of signals at θ_{AOA} and θ_{AOD} as shown in (2) and (3), where $\theta_{\text{AOD}} = \theta_{\text{AOA}} = \theta_{m,k}^{j,0}$ due to monostatic radar setting. The $s(t)$ is the transmitted sensing signal, and $\mathbf{z}(t)$ is the additive white Gaussian noise with zero mean and variance of σ^2 , i.e., $\mathbf{z}(t) \sim \mathcal{CN}(\mathbf{0}_{N_r}, \sigma^2 \mathbf{I}_{N_r \times 1})$.

$$\mathbf{b}(\theta_{\text{AOA}}) = \frac{1}{\sqrt{N_r}} [1, e^{-j\pi \cos(\theta_{\text{AOA}})}, \dots, e^{-j\pi(N_r-1) \cos(\theta_{\text{AOA}})}]^T. \quad (2)$$

$$\mathbf{a}(\theta_{\text{AOD}}) = \frac{1}{\sqrt{N_t}} [1, e^{-j\pi \cos(\theta_{\text{AOD}})}, \dots, e^{-j\pi(N_t-1) \cos(\theta_{\text{AOD}})}]^T. \quad (3)$$

The complex reflection coefficient $\beta_{m,k}^{j,0}$ is determined by the signal propagation distance and the radar cross section (RCS) of the ST, expressed as:

$$\beta_{m,k}^{j,0} = \frac{\epsilon_{m,k}^{j,0}}{(2d_{m,k}^{j,0})^2}, \quad (4)$$

where $d_{m,k}^{j,0}$ is the distance between the scatter and AP, and the RCS $\epsilon_{m,k}^{j,0}$ follows zero mean and unit variance Gaussian distribution.

The $\mathbf{f}^{j,0}$ represents the beamforming vector, which is written as:

$$\mathbf{f}^{j,0} = \mathbf{a}(\hat{\phi}_{(j,0)|(j-1,0)}^m), \quad (5)$$

where $\hat{\phi}_{(j,0)|(j-1,0)}^m$ represents the predicted angle of the center of ST based on estimated position and velocity of ST in the $\mathcal{F}_{j-1,0}$ sensing slot.

B. Sensing Measurement Model

We consider the classic radar processing technique, i.e., matched-filtering, to estimate the round-trip delay and Doppler frequency of the ST. This is implemented by correlating the received signal with the transmitted waveforms at different delays and performing an FFT, as in all radar signal processing, to generate Delay-Doppler maps. In this way, the moving target would be clearly distinguishable from clutter, which would normally appear closer to zero Doppler in the Delay-Doppler domain. The processed signal can be represented as:

$$\begin{aligned} \tilde{\mathbf{r}}_m^{j,0} &= \kappa \sqrt{p_m} \sum_{k=1}^K \beta_{m,k}^{j,0} \mathbf{b}(\theta_{m,k}^{j,0}) \mathbf{a}^\dagger(\theta_{m,k}^{j,0}) \mathbf{a}(\hat{\phi}_{(j,0)|(j-1,0)}^m) \\ &\quad \times \int_0^{\Delta T} s(t - \tau_{m,k}^{j,0}) s^*(t - \tau) e^{-j2\pi(\mu - \mu_{m,k}^{j,0})t} dt + \tilde{\mathbf{z}}_r \\ &= \kappa \sqrt{p_m} \sqrt{G} \sum_{k=1}^K \beta_{m,k}^{j,0} \mathbf{b}(\theta_{m,k}^{j,0}) \mathbf{a}^\dagger(\theta_{m,k}^{j,0}) \mathbf{a}(\hat{\phi}_{(j,0)|(j-1,0)}^m) \\ &\quad \times \bar{\delta}(\tau - \tau_{m,k}^{j,0}; \mu - \mu_{m,k}^{j,0}) + \tilde{\mathbf{z}}, \end{aligned} \quad (6)$$

where ΔT is the length of the sensing slot, and G represents the matched-filtering gain. The $\bar{\delta}(\tau; \mu)$ represents the normalized matched-filtering output function, which has a narrow mainlobe property in delay domain and Doppler domain to ensure high resolution, i.e., $\bar{\delta}(\tau; \mu) = 1$ when $\tau = 0$, and $\mu = 0$.

Therefore, the measured round-trip delay and Doppler frequency can be represented as:

$$\hat{\tau}_{m,k}^{j,0} = \frac{2d_{m,k}^{j,0}}{c} + z_{\tau_{m,k}^{j,0}}, \quad \hat{\mu}_{m,k}^{j,0} = \frac{2v_s \cos(\theta_{m,k}^{j,0}) f_c}{c} + z_{\mu_{m,k}^{j,0}}. \quad (7)$$

The $\theta_{m,k}^{j,0}$ can be estimated by the multiple signal classification (MUSIC) algorithm, whose measurements are expressed as

$$\hat{\theta}_{m,k}^{j,0} = \theta_{m,k}^{j,0} + z_{\theta_{m,k}^{j,0}}, \quad (8)$$

where the $z_{\tau_{m,k}^{j,0}}$, $z_{\mu_{m,k}^{j,0}}$ and $z_{\theta_{m,k}^{j,0}}$ are additive noises with zero means and variances of $\sigma_{\tau,j,m,k}^2$, $\sigma_{\mu,j,m,k}^2$, and $\sigma_{\theta,j,m,k}^2$.

Then the $\sigma_{\tau,j,m,k}^2$, $\sigma_{\mu,j,m,k}^2$, and $\sigma_{\theta,j,m,k}^2$ can be represented as:

$$\sigma_{i,j,m,k}^2 = \frac{a_i^2 \sigma^2}{p_m G |\kappa \beta_{m,k}^{j,0}|^2 |\varrho_{m,k}^{j,0}|^2}, i = \tau, \mu, \theta, \quad (9)$$

where $\varrho_{m,k}^{j,0} = \mathbf{a}^\dagger(\theta_{m,k}^{j,0}) \mathbf{a}(\hat{\phi}_{(j,0)|(j-1,0)}^m)$ represents the beamforming gain, and a_i are constants related to the system configuration, signal designs, and algorithms.

Finally, we can obtain the measurements of the coordinates of centroid, the angle of the centroid, and the velocity of the ST, which can be represented as

$$\begin{aligned} \hat{x}_{j,0} &= \frac{1}{MK} \sum_{m=1}^M \sum_{k=1}^K c \hat{\tau}_{m,k}^{j,0} \cos \hat{\theta}_{m,k}^{j,0} / 2, \\ \hat{y}_{j,0} &= \frac{1}{MK} \sum_{m=1}^M \sum_{k=1}^K c \hat{\tau}_{m,k}^{j,0} \sin \hat{\theta}_{m,k}^{j,0} / 2, \\ \hat{v}_{j,0} &= \frac{c}{2f_c} \frac{1}{M} \sum_{m=1}^M \frac{\sum_{k=1}^K \hat{\mu}_{m,k}^{j,0} \cos(\hat{\theta}_{m,k}^{j,0}) / \sigma_{\mu,j,m,k}^2}{\sum_{k=1}^K \cos^2(\hat{\theta}_{m,k}^{j,0}) / \sigma_{\mu,j,m,k}^2}. \end{aligned} \quad (10)$$

C. Communication Model

In the DMIMO setting, we denote the estimated communication channel between UE u and AP m in $\mathcal{F}_{j,n}$, $n \in \{1, \dots, N-1\}$ communication slot as $\hat{\mathbf{h}}_{u,m}^n \in \mathbb{C}^{N_u \times N_t}$. We assume a central server collects all the estimated channel $\hat{\mathbf{h}}_{u,m}^n \in \mathbb{C}^{N_u \times N_t}$ and stacks the channels between UE u and all the APs to obtain $\hat{\mathbf{h}}_u^{j,n} \in \mathbb{C}^{N_u \times MN_t}$. Without loss of generality, we consider the well-known zero-forcing (ZF) beamforming algorithm, where the complete estimated channel information is represented as $\hat{\mathbf{H}}^{j,n} = [\hat{\mathbf{h}}_1^{j,n}; \dots; \hat{\mathbf{h}}_U^{j,n}] \in \mathbb{C}^{UN_u \times MN_t}$. Therefore, the ZF beamforming weights $\mathbf{W}^{j,n}$ are calculated as

$$\mathbf{W}^{j,n} = \hat{\mathbf{H}}^{j,n \dagger} (\hat{\mathbf{H}}^{j,n} \hat{\mathbf{H}}^{j,n \dagger})^{-1}, \quad (11)$$

where $\mathbf{W}^{j,n} = [\mathbf{w}_1^{j,n}, \dots, \mathbf{w}_U^{j,n}] \in \mathbb{C}^{MN_t \times UN_u}$, and $\mathbf{w}_u^{j,n} = [\mathbf{w}_{u,1}; \dots; \mathbf{w}_{u,M}] \in \mathbb{C}^{MN_t \times N_u}$ represents the beamforming weights of each UE.

Then, considering a block fading channel model, we can present the received signal at UE u in each communication slot $\mathcal{F}_{j,n}$ as

$$\begin{aligned} \mathbf{y}_u^{j,n} &= \underbrace{\sqrt{p_u} \mathbf{h}_u^{j,n} \frac{\mathbf{w}_u^{j,n}}{\|\mathbf{w}_u^{j,n}\|_F} \mathbf{x}_u}_{\text{DesiredSignal}} + \\ &\quad \underbrace{\sum_{u' \in \mathcal{U} \setminus \{u\}} \sqrt{p_{u'}} \mathbf{h}_{u'}^{j,n} \frac{\mathbf{w}_{u'}^{j,n}}{\|\mathbf{w}_{u'}^{j,n}\|_F} \mathbf{x}_{u'}}_{\text{Interference}} + \mathbf{z}_u, \end{aligned} \quad (12)$$

where $p_u = M * p_m$ represents the allocated transmission power for each user in DMIMO setting, $\mathbf{x}_u \in \mathbb{C}^{N_u \times 1}$ represents the transmitted user data, and \mathbf{z}_u is the Gaussian noise with zero mean and σ^2 variance.

D. Problem Formulation

To enhance downlink transmission throughput in our considered DMIMO scenario, we aim to maximize the downlink throughput by optimizing the estimated channel state information, which can be formulated as follows:

$$\begin{aligned} \text{(OP1): } \max_{\hat{\mathbf{h}}_u^{j,n}} \sum_{j=1}^{\infty} \sum_{n=1}^N \sum_{u \in \mathcal{U}} \log 2 \det(\mathbf{R}_S^{u,j,n} + \mathbf{R}_I^{u,j,n}) \\ - \log 2 \det(\mathbf{R}_I^{u,j,n}), \end{aligned} \quad (13)$$

where

$$\mathbf{R}_S^{u,j,n} = p_u \mathbf{h}_u^{j,n} \frac{\mathbf{w}_u^{j,n} \mathbf{w}_u^{j,n \dagger}}{\|\mathbf{w}_u^{j,n}\|_F^2} \mathbf{h}_u^{j,n \dagger}, \quad (14)$$

and

$$\mathbf{R}_I^{u,j,n} = \sum_{u' \in \mathcal{U} \setminus \{u\}} p_{u'} \mathbf{h}_{u'}^{j,n} \frac{\mathbf{w}_{u'}^{j,n} \mathbf{w}_{u'}^{j,n \dagger}}{\|\mathbf{w}_{u'}^{j,n}\|_F^2} \mathbf{h}_{u'}^{j,n \dagger} + \sigma^2 \mathbf{I}. \quad (15)$$

III. SENSING-ASSISTED CHANNEL ESTIMATION FRAMEWORK

In this section, the proposed sensing-assisted channel estimation scheme will be presented. First, we consider that one sensing slot is allocated in each transmission frame to detect the position and velocity of the ST. Then, we utilize the estimated position of the ST to calculate the propagation paths between each AP and UE, where both LoS and NLoS propagation paths are considered via Ray-tracing method.

A. Multipaths Channel Model

We consider the channel between any AP m and the UE u comprises $L \geq 1$ paths, where the first one is the LoS path and the other $L-1$ paths are associated with the reflection of ST. Here, L satisfies $L \ll \min(N_u, N_t)$ in mmWave propagation, and only single-bounce reflections are considered. We assume the APs only perform channel estimation in each sensing slot, i.e., $\mathcal{F}_{j,0}$, where the estimated channel remains the same between two sensing slots, i.e., $\hat{\mathbf{h}}_{u,m}^{j,0} = \hat{\mathbf{h}}_{u,m}^{j,1} = \dots = \hat{\mathbf{h}}_{u,m}^{j,N-1}$.

Let $\hat{\theta}_{m,u,l}^{j,0}$ and $\hat{\theta}_{u,m,l}^{j,0}$, $0 \leq l \leq L$, be the estimated AOD and AOA of l^{th} communication path based on the estimated

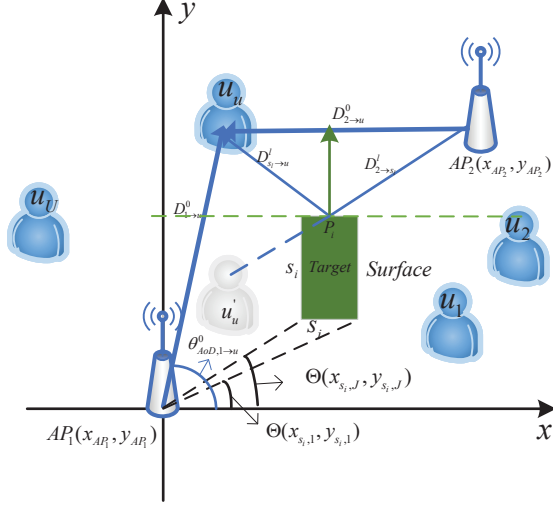


Fig. 2. Propagation reflection model between APs and UEs

ST position, where $l = 0$ represents the LoS path. Therefore, the channel coefficient between any AP m and the user u can be expressed as:

$$\hat{\mathbf{h}}_{u,m}^{j,0} = \sum_{l=0}^L I_{m \rightarrow u}^l \sqrt{N_t N_u} \hat{\alpha}_{m \rightarrow u}^l \mathbf{c}(\hat{\theta}_{u,m,l}^{j,0}) \mathbf{a}(\hat{\theta}_{m,u,l}^{j,0})^\dagger, \quad (16)$$

where

$$\mathbf{c}(\theta_{\text{AOA}}) = \frac{1}{\sqrt{N_u}} [1, e^{-j\pi \cos(\theta_{\text{AOA}})}, \dots, e^{-j\pi(N_u-1) \cos(\theta_{\text{AOA}})}]^T. \quad (17)$$

It is noted that $I_{m \rightarrow u}^l = 1$ indicates the propagation path l exists, otherwise not. In the following sections, we will present how to calculate the propagation gain $\hat{\alpha}_{m \rightarrow u}^l$ under the condition of the LoS path and NLoS path.

B. LoS Path

It is noted that the mobility of the ST causes variations of communication links between UEs and APs, and may lead to blockage of the LoS path. Therefore, the existence of LoS path is determined based on the estimated position of ST in (10) and prior width w_s and length l_s information.

The LoS paths between APs and UE exist only if the ST is not blocking the communication link, i.e., they are not blocked by any surface of the ST, like the LoS link between AP AP_1 and UE u_u shown in Fig. 2, where four surfaces of the ST are represented as $\{s_i, i = 1, 2, 3, 4\}$. As shown in Fig. 2, each surface can induce an angular range defined as

$$\Omega_{s_i} = \begin{cases} [\Theta(x_{s_i,1}, y_{s_i,1}), \Theta(x_{s_i,J}, y_{s_i,J})], \\ \Theta(x_{s_i,1}, y_{s_i,1}) < \Theta(x_{s_i,J}, y_{s_i,J}) \\ [\Theta(x_{s_i,1}, y_{s_i,1}), 2\pi) \cup [0, \Theta(x_{s_i,J}, y_{s_i,J})], \\ \Theta(x_{s_i,1}, y_{s_i,1}) > \Theta(x_{s_i,J}, y_{s_i,J}). \end{cases} \quad (18)$$

where $\Theta(x_{s_i,1}, y_{s_i,1}), \Theta(x_{s_i,J}, y_{s_i,J})$ are the angles of the two endpoints of the surface s_i . The calculation of $\Theta(x, y)$ can be found in [12].

Therefore, the LoS paths exist, i.e., $I_{m \rightarrow u}^0 = 1$, if and only if $\Theta(x_u, y_u)$ does not fall within any range $\Omega_{s_i}, i = \{1, 2, 3, 4\}$.

Then, the corresponding propagation gain of the LoS path $\hat{\alpha}_{m \rightarrow u}^0$ is calculated as:

$$\hat{\alpha}_{m \rightarrow u}^0 = e^{j \frac{2\pi D_{m \rightarrow u}^0}{\lambda}} \sqrt{\min\left(\frac{A_u^0}{W(\hat{\theta}_{m,u,0}, N_t) D_{m \rightarrow u}^0}, 1\right)}, \quad (19)$$

$$D_{m \rightarrow u}^0 = \sqrt{(\hat{x}_u - x_m)^2 + (\hat{y}_u - y_m)^2}$$

where A_u^0 is the effective user aperture $A_u^0 = \lambda + (N_u - 1)\lambda |\sin(\hat{\theta}_{u,m,0})|$, and $D_{m \rightarrow u}^0$ is the estimated distance between the AP m and the user u .

C. NLoS Path

Considering the reflective (i.e., NLoS) paths caused by ST, the NLoS path exists, i.e., $I_{m \rightarrow u}^l = 1$, if and only if the AP and the mirror UE u'_u over the surface s_i have an interaction point, and the reflective path is not blocked by any other surfaces. For instance, in Fig. 2, one NLoS link exists between AP_2 and UE u_u with the reflection point P_i on surface s_i . Therefore, the reflection coefficient (propagation gain) $\hat{\alpha}_{m \rightarrow u}^l$ can be calculated as (20).

In (20), $D_{m \rightarrow s_i}^l$ and $D_{s_i \rightarrow u}^l$ are the distances from the reflection surface s_i to the AP m and the user u , and $\{\hat{\Phi}_{s_i}^l, \hat{R}_s^l, \hat{R}_d^l\}$ denotes the reflection property of the reflective surface. $\hat{\Phi}_{s_i}^l$ is the phase shift determined by the reflection property, $\hat{R}_s^l \in (0, 1)$ and $\hat{R}_d^l \in (0, 1)$ are the specular reflectance and diffuse reflectance of the reflective surface, respectively.

TABLE I
SIMULATION PARAMETERS

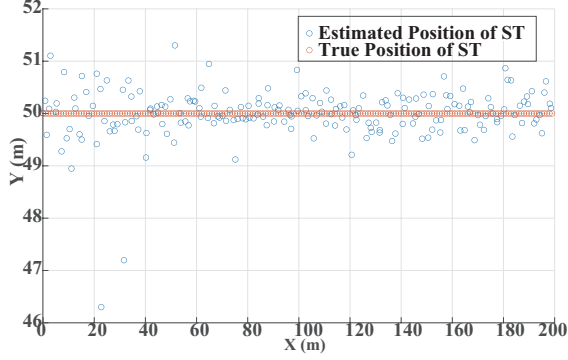
Number of APs M	5
Number of UEs U	3
Frequency f_c	60GHz
Slot Length ΔT	50 ms
Transmission Frame	0.5 s
Transmission Power of UEs	23 dBm
Bandwidth	500 MHz
Transmission Power of APs p_m	23 dBm
Number of Transmitting Antennas in AP N_t	32
Number of Receiving Antennas in AP N_r	32
Number of Antennas in UE N_u	4
ST Moving Speed v_s	2 m/s
ST Length l_s	5 m
ST Width w_s	2 m
Number of Scatters K	8
Noise power σ^2	-87 dBm
a_τ	$6.7 * 10e^{-7}$
a_μ	$2 * 10^4$
a_θ	1

IV. SIMULATION RESULTS

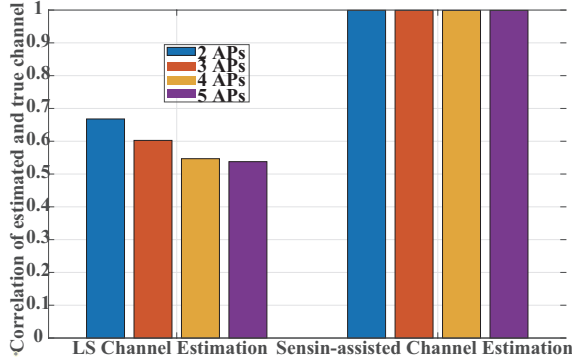
In this section, we evaluate the performance of our proposed sensing-assisted channel estimation framework, and compare it against the traditional LS channel estimation method. The indoor scenario is modeled as a 200m square, where the left bottom is the original point, i.e., $O(0, 0)$. Five APs are deployed at $AP_1(0, 0)$, $AP_2(200, 200)$, $AP_3(0, 200)$, $AP_4(200, 0)$, and $AP_5(100, 200)$ respectively. Three UEs are deployed at $u_1(50, 150)$, $u_2(150, 150)$, and $u_3(150, 100)$, respectively. We assume the moving target ST moves towards the

$$\begin{aligned} \hat{\alpha}_{m \rightarrow u}^l &= e^{-j(\hat{\Phi}_{s_i}^l - \frac{2\pi(D_{m \rightarrow s_i}^l + D_{s_i \rightarrow u}^l)}{\lambda})} \\ &\times \sqrt{\eta \left(\min \left(\frac{A_u^l}{W(\hat{\theta}_{m,u,l}, N_t)(D_{m \rightarrow s_i}^l + D_{s_i \rightarrow u}^l)}, 1 \right) \hat{R}_s^l + \frac{\sin^2 \left(\Theta(\frac{1}{a_l}, 1) - \Theta(x_{m \rightarrow u}^l, y_{m \rightarrow u}^l) \right) A_u^l}{\sqrt{4(D_{s_i \rightarrow u}^l)^2 + A_u^l{}^2}} \hat{R}_d^l \right)}, \\ D_{m \rightarrow s_i}^l &= \sqrt{(x_{s_i}^l - x_m)^2 + (y_{s_i}^l - y_m)^2}, \quad D_{s_i \rightarrow u}^l = \sqrt{(x_{s_i}^l - x_u)^2 + (y_{s_i}^l - y_u)^2}. \end{aligned} \quad (20)$$

x-axis positive direction with the speed of 2m/s starting from $O_t(0, 50)$. It is noted that the length and width of the moving target are 5m and 2m, respectively. Detailed parameters are given in Table. I.



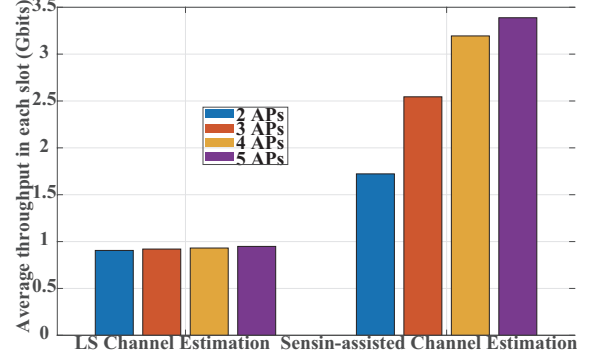
(a) Estimated position and ground truth position of ST



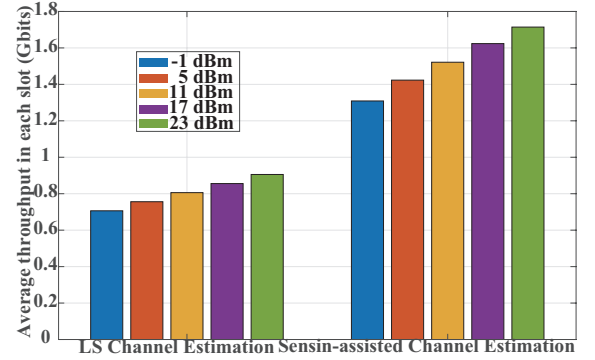
(b) Correlation between estimated channel and ground truth channel under various number of APs

Fig. 3. Estimated position of ST and channel correlation coefficient

Fig. 3 illustrates the estimated positions of ST, and channel correlation coefficient in traditional LS and sensing-assisted channel estimation. In Fig. 3 (a), we can observe that multiple APs successfully estimate and track the position of ST, where the mean estimation error is 0.37m. In Fig. 3 (b), we present the correlation coefficient between the estimated channel and ground truth channel, which is calculated as $\frac{1}{U} \sum_{u \in \mathcal{U}} \frac{\text{trace}(\mathbf{h}_u^{j,n} \mathbf{h}_u^{j,n \dagger})}{\|\mathbf{h}_u^{j,n}\|_F \|\mathbf{h}_u^{j,n}\|_F}$ to quantify the correlation between ground truth paths and estimated paths. We can observe that the proposed sensing-assisted channel estimation scheme achieves over 0.99 correlation coefficient between the estimated channel and ground truth channel, where the correlation coefficient of LS channel estimation only achieves 0.6 correlation coefficient and decreases with the increasing number of APs, due to the increase of channel dimension.



(a) Average throughput under various number of APs



(b) Average throughput under various transmission power of APs

Fig. 4. Average throughput under various numbers of APs and transmission power.

Fig. 4 illustrates the average throughput in each slot for varying number of APs and various transmission powers. In Fig. 4 (a), we can observe that the average throughput increases significantly with the increasing number of APs for the proposed sensing-assisted channel estimation framework. However, increasing the number of APs does not significantly increase the throughput gain in the traditional LS estimation. This is because the DMIMO with a higher number of APs requires stringent channel estimation accuracy for interference mitigation, which cannot be satisfied by the traditional LS estimation. In Fig. 4 (b), we can observe that the average throughput of both LS estimation and sensing-assisted estimation increases with increasing APs' transmission power. However, this increase is more pronounced with the proposed method.

V. CONCLUSION

In this paper, we proposed a sensing-assisted channel estimation framework, which exploits the sensing capability

of multiple APs in a DMIMO network to enhance channel estimation performance via the Ray-tracing method. Different from the traditional sensing-assisted communication works focusing on LoS scenarios, the proposed scheme can accurately estimate the NLoS user channel in a dynamic environment caused by the moving targets, which achieves significant throughput performance gain compared to the traditional LS estimation.

REFERENCES

- [1] A. Liu, Z. Huang, M. Li, Y. Wan, W. Li, T. X. Han, C. Liu, R. Du, D. K. P. Tan, J. Lu *et al.*, "A survey on fundamental limits of integrated sensing and communication," *IEEE Communications Surveys & Tutorials*, vol. 24, no. 2, pp. 994–1034, 2022.
- [2] U. Demirhan and A. Alkhateeb, "Cell-free ISAC mimo systems: Joint sensing and communication beamforming," *IEEE Transactions on Communications*, pp. 1–1, 2024.
- [3] Z. Liu, J. Zhang, Z. Liu, H. Du, Z. Wang, D. Niyato, M. Guizani, and B. Ai, "Cell-free XL-MIMO meets multi-agent reinforcement learning: Architectures, challenges, and future directions," *IEEE Wireless Communications*, 2024.
- [4] J. Mu, Y. Gong, F. Zhang, Y. Cui, F. Zheng, and X. Jing, "Integrated sensing and communication-enabled predictive beamforming with deep learning in vehicular networks," *IEEE Communications Letters*, vol. 25, pp. 3301–3304, 10 2021.
- [5] L. Cazzella, M. Mizmizi, D. Tagliaferri, D. Badini, M. Matteucci, and U. Spagnolini, "Deep learning-based target-to-user association in integrated sensing and communication systems," *IEEE Journal of Selected Topics in Signal Processing*, vol. 18, no. 5, pp. 886–900, 2024.
- [6] S. Huang, M. Zhang, Y. Gao, and Z. Feng, "Mimo radar aided mmwave time-varying channel estimation in mu-mimo v2x communications," *IEEE Transactions on Wireless Communications*, vol. 20, pp. 7581–7594, 11 2021.
- [7] F. Liu, Y. Cui, C. Masouros, J. Xu, T. X. Han, Y. C. Eldar, and S. Buzzi, "Integrated sensing and communications: Toward dual-functional wireless networks for 6g and beyond," *IEEE Journal on Selected Areas in Communications*, vol. 40, pp. 1728–1767, 6 2022.
- [8] S. Lu, F. Liu, Y. Li, K. Zhang, H. Huang, J. Zou, X. Li, Y. Dong, F. Dong, J. Zhu, Y. Xiong, W. Yuan, Y. Cui, and L. Hanzo, "Integrated sensing and communications: Recent advances and ten open challenges," *IEEE Internet of Things Journal*, pp. 1–1, 2024.
- [9] C. Jiao, Z. Zhang, C. Zhong, and Z. Feng, "An indoor mmwave joint radar and communication system with active channel perception," in *2018 IEEE International Conference on Communications (ICC)*. IEEE, 2018, pp. 1–6.
- [10] Q. Zhang, H. Sun, X. Gao, X. Wang, and Z. Feng, "Time-division isac enabled connected automated vehicles cooperation algorithm design and performance evaluation," *IEEE Journal on Selected Areas in Communications*, vol. 40, no. 7, pp. 2206–2218, 2022.
- [11] Z. Du, F. Liu, W. Yuan, C. Masouros, Z. Zhang, S. Xia, and G. Caire, "Integrated sensing and communications for v2i networks: Dynamic predictive beamforming for extended vehicle targets," *IEEE Transactions on Wireless Communications*, vol. 22, no. 6, pp. 3612–3627, 2023.
- [12] C. Jiao, Z. Zhang, C. Zhong, X. Chen, and Z. Feng, "Millimeter wave communication with active ambient perception," *IEEE Transactions on Wireless Communications*, vol. 18, no. 5, pp. 2751–2764, 2019.